Radiology

"In Press" papers have undergone full peer review and have been accepted for publication in Radiology. This article will undergo copyediting, layout, and proof review before it is published in its final version. Please note that during production of the final copyedited article, errors may be discovered which could affect the content.

Chest CT Findings in Hospitalized Patients with SARS-CoV-2: Delta versus Omicron Variants

Manuscript type: Original Research

Soon Ho Yoon, MD, PhD[1, *] Jong Hyuk Lee, MD, PhD[1, *] Baek-Nam Kim, MD[2, †]

[1]Department of Radiology, Seoul National University Hospital, Seoul National University College of Medicine, 101, Daehak-ro, Jongno-gu, Seoul, 03080, Korea; [2]Department of Internal Medicine, Inje University Sanggye Paik Hospital, Inje University College of Medicine, Seoul, 01757, Korea.

†Address correspondence to:

Baek-Nam Kim, MD. Department of Internal Medicine, Inje University Sanggye Paik Hospital, Inje University College of Medicine, Seoul, 01757, Korea.

E-mail: kimbn@paik.ac.kr

***S.H.Y. and J.H.L. contributed equally to this work.**

In press

This copy is for personal use only. To order printed copies, contact *reprints@rsna.org*

Funding information

This work was supported by the Korea Medical Device Development Fund grant funded by the Korea government (the Ministry of Science and ICT, the Ministry of Trade Industry and Energy, the Ministry of Health & Welfare, Republic of Korea, the Ministry of Food and Drug Safety) (Project Number: 202011A03).

Conflicts of interest

Activities related to the present article: S.H.Y. is a chief medical officer for Medical IP, and holds stock option in Medical IP.

In press

Abbreviations

BV5 = pulmonary blood volume for vessels smaller than 5 mm^2 in cross section

RSNA = Radiological Society of North America

GGO = ground-glass opacity

Summary statement

The Omicron SARS-CoV2 variant showed more frequent nontypical CT findings (peri-bronchovascular predilection, less pulmonary vascular involvement) than the Delta variant in hospitalized patients with COVID-19 disease with comparable CT severity.

Key Results

- Only 32% of patients with the Omicron SARS-CoV-2 variant had typical ground-class opacity at CT versus 57% of those with Delta variant (*P*=.001);
- Peri-bronchovascular predilection was greater for Omicron versus Delta variant (38% vs 7%; *P* <.001, respectively).
- Pneumonia extent (*P* =.17) and volume (*P* =.67) were not different between the variants after adjusting for confounders of age, comorbidities, vaccination, and infection duration.

In press

Abstract

Background: CT manifestations of severe acute respiratory syndrome coronavirus-2 (SARS-CoV-2) may differ among variants.

Purpose: To compare the chest CT findings of SARS-CoV-2 between the Delta and Omicron variants.

Materials and Methods: This retrospective study collected consecutive baseline chest CT images of hospitalized patients with SARS-CoV-2 from a secondary referral hospital when the Delta and Omicron variants predominated. Two radiologists categorized CT images based on the Radiological Society of North America classification system for coronavirus disease 2019 (COVID-19) and visually graded pneumonia extent. Pneumonia, pleural effusion, and intrapulmonary vessels were segmented and quantified on CT images using *a priori* developed neural networks, followed by reader confirmation. Multivariable logistic and linear regression analyses were performed to examine the associations between the variants and CT category, distribution, severity, and peripheral vascularity.

Results: In total, 88 patients with the Delta (mean age, 67 years±15; 46 men) and 88 patients with the Omicron (mean age, 62 years±19; 51 men) variants were included. Omicron was associated with a less frequent typical peripheral, bilateral ground-glass opacity (32% [28/88] versus 57% [50/88]; *P*=.001), more frequent peri-bronchovascular predilection (38% [25/66] versus 7% [5/71]; *P*<.001), lower visual pneumonia extent (5.4±6.0 versus 7.7±6.6; *P*=.02), similar pneumonia volume (5%±10 versus 7%±11; *P*=.14), and a higher proportion of vessels with a cross-sectional area smaller than 5 mm^2 relative to the total pulmonary blood volume (BV5%; 48%±11 versus 44%±8; *P*=.004). In adjusted analyses, Omicron was associated with a non-typical appearance (odds ratio, 0.34; *P*=.006), peri-bronchovascular predilection (odds ratio, 9.2; *P*<.001), and higher BV5% (β value, 3.8; *P*=.01) but similar visual pneumonia extent

In press

(*P*=.17) and pneumonia volume (*P*=.67) relative to Delta variant.

Conclusions: On chest CT, the Omicron SARS-COV-2 variant showed nontypical, peribronchovascular pneumonia and less pulmonary vascular involvement than the Delta variant in hospitalized patients with comparable CT disease severity.

In press

Introduction

Since the coronavirus disease 2019 (COVID-19) pandemic began, severe acute respiratory syndrome coronavirus-2 (SARS-CoV-2) has evolved through genetic mutations during viral replication (1, 2). Several variants of SARS-CoV-2 have been reported worldwide throughout the pandemic, and some variants are classified as variants of concern due to increased transmissibility, disease severity, or evasiveness of treatments and vaccines (3). The Delta and Omicron variants are the two latest variants of concern (4, 5).

The Delta variant was first identified in India in December 2020 and became the globally dominant strain in June 2021. This variant of concern has mutations that make it highly transmissible (more than 60% higher transmissibility than the previous variant), less responsive to antibodies and treatment (i.e., reduced neutralization by antibodies generated against previous infection or vaccination), and more likely to cause adverse outcomes (e.g., severe cases, hospitalization, deaths) (6). Indeed, the Delta variant caused the second wave of India's pandemic and subsequent waves in other countries (7). The Omicron variant, which was first reported in November 2021 in South Africa, was designated as another variant of concern and has become the dominant strain following the Delta variant in most countries. Although the Omicron variant has up to 3.7 times higher transmissibility than the Delta variant, it is regarded as less virulent in terms of the rate of hospitalization, intensive care unit admissions, and mortality (8-10).

Chest CT plays a key role in the diagnosis, detection of complications, and potential prognostication of patients with COVID-19 (11, 12). Prior studies have investigated differences between these two contiguously emerging dominant variants with a focus on their spike proteins, diagnostic tests, clinical characteristics, transmissibility, and outcomes (9, 10, 13). However, it remains underexplored whether the CT findings of COVID-19 differ among

In press

variants. This study aimed to compare the chest CT findings of COVID-19 between the Delta and Omicron variants.

In press

Materials and Methods

The institutional review board approved this retrospective study and waived informed consent (IRB No. SGPAIK 2022-03-009).

Study sample

This study was conducted at one of the secondary referral hospitals for the treatment of patients with mild-to-moderate COVID-19, which operated thirty beds for COVID-19. Inclusion criteria corresponded to patients with a) polymerase chain reaction assay-proven SARS-CoV-2 AND b) mild (no requirement for oxygen treatment) to moderate (a necessity for oxygen treatment with nasal prong or facial mask) severity at admission AND c) any following risk factors for progression (Appendix E1). Exclusion criteria corresponded to a) patients necessitating intensive care unit care or ventilator support at admission, b) pregnant women, and c) patients who chose not to undergo CT scanning.

The hospital routinely performed baseline CT images for hospitalized patients. We collected consecutive baseline CT images in November 2021 and February 2022 (Fig E1) when the Delta and Omicron variants predominated in Korea, accounting for 99% and 97% of cases, respectively (14). All chest CT scans were obtained at full inspiration using one of the following 24- or higher-channel CT scanners (Appendix E1).

We collected clinico-laboratory information, including on infection duration at the time of the CT scan (i.e., days from symptom onset to the CT scan) (15). The composite outcome was the occurrence of any following events: oxygen ventilation, intensive care unit admission, and mortality.

In Press

Visual CT analysis

The randomly assigned baseline CT examinations were independently evaluated by two board-certified thoracic radiologists (S.H.Y. and J.H.L., with 17 and 10 years of clinical experience in thoracic imaging, respectively). They were blinded to the patient's clinical information, including the variant and dates of CT examinations, other than the fact that the patient was infected with SARS-CoV-2. Disagreement between two radiologists were resolved by consensus.

COVID-19 pneumonia CT images were classified into the four categories according to the Radiological Society of North America (RSNA) Expert Consensus Document (16): typical appearance, indeterminate appearance, atypical appearance, negative for COVID-19 pneumonia, developed during the first wave of SARS-CoV2 (Appendix E1). For example, typical features of COVID-19 pneumonia typically include ground glass opacities (GGO) with or without consolidation in a peripheral, posterior, and diffuse or lower lung zone distribution, GGO with round morphology or a "crazy paving" pattern. Bronchial wall thickening, mucoid impactions, and nodules ("tree-in-bud" and centrilobular) seen commonly in infections, are not typically observed.

Pneumonia extent was visually assessed using a scale of 0 to 5 for each of the five lung lobes (17): 0, indicating no involvement; 1, less than 5% involvement; 2, 5%–25% involvement; 3, 26%–49% involvement; 4, 50%–75% involvement; and 5, more than 75% involvement. The total CT score was the sum of the individual lobar scores and ranged from 0 (no involvement) to 25 (maximum involvement). The radiologists also assessed pneumonia density, predilected distribution (bronchovascular versus subpleural), lymphadenopathy, and pleural effusion (Appendix E1).

In press

Quantitative CT analysis

The CT images were processed using commercially available segmentation software (MEDIP PRO v2.0.0.0; MEDICALIP, Seoul, Korea) using *a priori* developed deep neural networks for segmenting the lung (18), COVID-19 pneumonia (19), pulmonary lobes and fissures, pulmonary vessels (20), and pleural effusion (https://cris.nih.go.kr/cris/search/detailSearch.do/20687): The networks were updated with 3DnnU-Net (21), and the dice similarity scores for those structures were 0.99 (lung), 0.84 (COVID-19), 0.98 (lobes), 0.91 (vessels), and 0.90 (effusion) in internal datasets.

A chest radiologist (S.H.Y.) reviewed and confirmed the segmentation masks. If any corrections were required, an imaging technician manually adjusted the masks under the instruction of the radiologist. The radiologist and technician were blinded to any clinical information other than the fact that the patients were infected with COVID-19. The volume (mL) of the segmented lung parenchymal and pneumonia masks was quantified to determine the proportion of COVID-19 pneumonia in the entire lung parenchyma and each lobe. The mean CT attenuation of COVID-19 was also calculated and converted into pneumonia weight (grams) using an equation based on the CT attenuation and pneumonia volume (22). BV5% was calculated as the percentage of blood volume in intrapulmonary vessels with a cross-sectional area <5 mm^2 relative to the total pulmonary blood volume (20). Lower BV5% reflected endothelial dysfunction and loss of microvasculature in COVID-19 (23, 24). The volume of pleural effusion was quantified in milliliters if present.

Statistical analysis

In press

Categorical variables were compared using the Fisher's exact and the χ^2 tests, and continuous variables were compared using the *t* test or Mann-Whitney *U* test. Inter-reader agreements for visual assessment and total CT score were evaluated using Cohen's kappa coefficient (κ) and intraclass correlation coefficient, respectively.

We examined the correlation between visual CT extent and pneumonia volume using the Pearson correlation coefficient. Multivariable logistic regression analysis was performed to examine the association of the variants with CT category and peri-bronchovascular predilection. Multivariable linear regression analyses were performed to examine the relationships between the variants and visual CT extent, pneumonia percentage, weight with the same adjustment. Multivariable Cox regression analyses were conducted to evaluate the association between the variants and the composite outcome. All multivariable analyses were conducted using an input function of confounders (Appendix E1). Infection duration was classified into five categories: 1, pre-symptomatic; 2, 0-2 days; 3, 3-5 days; 4, 6-11 days; 5, >11 days (15).

The statistical analyses were conducted using SPSS software (version 25.0, IBM), and a two-sided *P*-value <.05 was considered statistical significance.

In press

Results

Clinical Characteristics of the Study Sample

Of 187 hospitalized patients with SARS-CoV-2, after 11 patients were excluded due to pregnancy (n=8) and reluctance for CT examinations (n=3), the final study sampled was 176. Of the 176 patients, 88 and other 88 patients had the Delta (46 men and 42 women; mean age, 67 years ± 15 [standard deviation]) and Omicron variants (51 men and 37 women; mean age, 62 years ± 19), respectively. All patients denied a prior infection with SARS-CoV-2. A flow diagram is given in Fig 1, and the clinical characteristics of this study sample are described in Table 1.

Patients with the Omicron variant had higher levels of vaccination than those with the Delta variant (unvaccinated: 28% [25 of 88] versus 32% [28 of 88]; partially vaccinated: 5% [4 of 88] versus 6% [5 of 88]; fully vaccinated: 23% [20 of 88] versus 62% [55 of 88]; booster vaccinated: 44% [39 of 88] versus 0% [0 of 88]; $P<.001$). The interval between symptom onset and CT scans was shorter in patients with the Omicron variant than those with the Delta variant (3.9 days ± 3.2 versus 5.5 days ± 4.5; $P=.01$) in symptomatic patients. Other clinical characteristics, including age, sex, comorbidities, the proportion of asymptomatic patients at the time of CT scans, white blood cell count, lymphocyte count, lactate dehydrogenase, the proportion of patients requiring oxygen treatment, and the proportion of unfavorable outcomes did not show evidence of a difference between the two variants (all *P*-values >.05) (Table 1).

Visual Assessment and Quantitative Assessment

In press

The CT findings of the Omicron and Delta variants are described in Table 2. In terms of the RSNA COVID-19 imaging classification, the Omicron and Delta variants had different appearances (the proportions of typical, indeterminate, atypical appearance, and negative for pneumonia were 32% [28 of 88], 31% [27 of 88], 13% [11 of 88], and 25% [22 of 88] in patients with the Omicron variant; and 57% [50 of 88], 20% [18 of 88], 3% [3 of 88], and 19% [17 of 88] in patients with the Delta variant; *P*=.004). When dichotomizing appearance as typical or non-typical, the Omicron variant presented the typical CT appearance of COVID-19 pneumonia less frequently than the Delta variant (32% [28 of 88] versus 57% [50 of 88]; *P*=.001). The visual score of pneumonia extent was lower in patients with the Omicron variant (mean score, 5.4±6.0) than in those with the Delta variant (mean score, 7.7±6.6; *P*=.02). However, no evidence of differences were found between the two variants in the CT findings of visual assessment of pneumonia density (predominant GGO, predominant consolidation, and mixed pattern: 68% [45 of 66], 12% [8 of 66], and 20% [13 of 66], respectively, in the Omicron variant versus 66% [47 of 71], 8% [6 of 71], and 25% [18 of 71], respectively, in the Delta variant; P=.61), the presence of lymphadenopathy (11% [10 of 88] versus 15% [13 of 88]; *P*=.66), and pleural effusion (18% [16 of 88] versus 22% [19 of 88]; *P*=.71).

Regarding inter-reader agreement for visual assessment of CT findings of the two variants, Cohen's kappa coefficients ranged from 0.51 to 0.81 with the highest value of 0.81 (95% confidence interval [CI]: 0.74, 0.88) for RSNA COVID-19 imaging classification and the lowest value of 0.51 (95% CI: 0.41, 0.61) for pneumonia density. The intraclass correlation coefficient for pneumonia extent was 0.98 (95% CI: 0.98, 0.99).

In the quantitative CT analysis, patients with the Omicron variant had a higher BV5% than those with the Delta variant (48% ± 11 versus 44% ± 8; *P*=.004). The mean CT value (-404 HU ± 139 versus -402 HU ± 115; *P*=.92), quantitative analysis of pneumonia extent (5%

In press

± 10 versus 7% ± 11; *P*=.14), pneumonia weight (95g ± 174 versus 143g ± 191; *P*=.09), and pleural effusion amount (275 mL ± 407 versus 149 mL ± 264; *P*=.47) showed no evidence of differences between the two variants (Fig 2, Fig 3, Fig 4, and Fig 5). The Pearson correlation coefficient between visual pneumonia extent and pneumonia volume was .84.

Univariable and Multivariable Analyses for Impact of Omicron Compared to Delta variant

In the univariable analyses, the Omicron variant had a lower frequency of a typical CT appearance (odds ratio, 0.36; *P*=.001), a more frequent peri-bronchovascular predilection (odds ratio, 8.0; *P*<.001), a lower visual pneumonia extent (β value, -2.3; *P*=.02), and greater BV5% (β value, 4.4; *P*=.004) than the Delta variant, whereas pneumonia volume (β value, -2.3; *P*=.14), pneumonia weight (β value, -47; *P*=.17). 30-day composite outcomes were comparable between the variants (hazard ratio, 1.8; *P*=.21) (Table 3).

The multivariable analyses after adjusting for confounders confirmed that Omicron had a less frequent typical CT appearance (odds ratio, 0.34; 95% CI: 0.16, 0.74; *P*=.006), a more frequent peri-bronchovascular predilection (odds ratio, 9.2; 95% CI: 2.9, 28; *P*<.001), and a greater BV5% (β value, 3.8; 95% CI: 0.92, 6.8; *P*=.01) relative to Delta variant. After adjustment, there were no evidence of differences between the Omicron and Delta variants regarding visual pneumonia extent (β value, -1.09; *P*=.17), pneumonia volume (β value, -0.62; *P*=.67), pneumonia weight (β value, -6.9; *P*=.82), and 30-day composite outcomes (hazard ratio, 3.1; *P*=.11; hazard ratio: 2.4; *P*=.29).

Statistically significant confounders were identified in the multivariable analyses: the proportion of patients with a typical CT appearance also was greater with age (*P*=.006) and an

In press

infection duration of six days or longer (*P*<.001 to .004), while it was lower with full vaccination status (*P*=.006). The visual extent, pneumonia volume, and pneumonia weight also was greater with age (*P*<.001 to .009) and a longer infection duration (all *P*-values <.001), but was lower with full vaccination (*P*<.001 to 0.08). The BV5% was lower as pneumonia volume was greater (*P*=.001). CT severity was predictive of developing the 30-day composite outcome regardless of whether it was assessed visually or quantitatively (*P*=.002 for both).

In press

Discussion

The CT manifestations of COVID-19 among different variants remains underexplored. We found that Omicron variant was associated with a smaller proportion of patients with a typical CT appearance (32% [28 of 88] versus 57% [50 of 88]; *P*=.001), a larger proportion of patients with peri-bronchovascular pneumonia (38% [25/66] versus 7% [5/71]; *P*<.001), a lower visual pneumonia extent (5.4 ± 6.0 versus 7.7 ± 6.6; *P*=.02), similar pneumonia volume (5% ± 10 versus 7% ± 11; *P*=.14), and a higher proportion of vessels with a cross-sectional area smaller than 5 mm^2 relative to the total pulmonary blood volume (BV5%; 48% ± 11 versus 44% ± 8; *P*=.004). When adjusted for confounders including age, comorbidities, vaccination, and infection duration, the Omicron variant was associated with a non-typical appearance (odds ratio, 0.34; *P*=.006), peri-bronchovascular predilection (odds ratio, 9.2; *P*<.001) and higher BV5 (β value, 3.8; *P*=.01) but not with visual pneumonia extent (β value, -1.09; *P*=.17) or pneumonia volume (β value, -0.62; *P*=.67).

The frequency of a typical CT appearance has been reported to vary from 17% to 53% depending on the site and clinical indication (25-28), but our study sample with both variants underwent chest CT at the same site and for the same indications. Similar proportions of patients with both variants were unvaccinated or partially vaccinated, and these patients might be more likely to have a typical CT appearance (29). The Omicron's odds of manifesting with a typical CT appearance and peri-bronchovascular predilection remained significant, even after adjusting for those confounders. The Omicron variant replicates better in the bronchi but worse in the lung parenchyma (13), and these characteristics may hinder Omicron from presenting a typical CT appearance when pneumonia is established in the lung parenchyma, while promoting peri-bronchovascular predilection.

BV5%, which reflects peripheral pulmonary volume and accounts for the majority of

In press

pulmonary blood volume (30), has been found to be lower in patients with SARS-CoV-2 than in healthy individuals and patients with acute respiratory distress syndrome (23, 24). Furthermore, a lower BV5% was identified as a predictor of adverse clinical outcomes in COVID-19 (31). This characteristic reduction of BV5% in COVID-19 could result from SARS-CoV-2-induced vasoconstriction or microthrombi of small-caliber vessels (24). Indeed, SARS-CoV-2 pathologically inflames small vessels, provokes thrombi (32, 33), and leads to frequent in-situ pulmonary thrombosis, especially in severe cases (34). Interestingly, early observations suggested that the Omicron variant might have a lower thrombosis rate than previous variants (35). This potentially provides support for the possibility that Omicron might involve fewer pulmonary vessels, in line with there being less involvement of the lower respiratory system.

Lower BV5% and CT vascular engorgement seem to result from the same vascular pathologies of COVID-19 but manifest at different pulmonary vascular calibers. BV5%'s cross-sectional vessel area corresponds to a vascular diameter smaller than 1.26 mm given the equation for a circle. These peripheral minute vessels had vasoconstriction or thrombosed but are too small to be visually assessed on CT. Meanwhile, vascular engorgement in COVID-19 was typically observed in segmental or subsegmental vessels. The diameters were 3-4 mm or larger, corresponding to a cross-sectional vessel area 28-50 mm^2 or larger. Vascular engorgement can reflect vascular dilatation or thrombosis proximal to SARS-CoV2-affected microvessels. Taken together, modern CT provided a multi-level analysis for revealing pulmonary vascular pathology in COVID-19 from impaired perfusion (below millimeter), lower peripheral BV5% (around millimeter), and proximally engorged vascular changes (over millimeter).

Our study had limitations. This study was retrospective and only included a relatively small number of hospitalized patients. In addition, patient inclusion was conducted without

In press

calculating the sample size. Participants did not undergo testing to confirm the SARS-CoV-2 variant. Third, the clinical severity of hospitalized patients might not have been identical between variants, and the number of COVID-19 cases remained low in November 2021 (when the Delta variant predominated), but soared in February 2022 (Omicron variant). Fourth, the pulmonary vessels could not be segmented in dense consolidation areas on non-contrast CT images as the neural network and radiologist could not trace the vessels within consolidations. Fifth, we did not adjust for the multiplicity of tests in our analyses.

In conclusion, the Omicron variant showed more frequent non-typical, peri-bronchovascular pneumonia and less pulmonary vascular involvement than the Delta variant in hospitalized patients with comparable CT severity. The CT characteristics of Omicron may hamper radiologists from promptly recognizing COVID-19 on CT images when incidentally encountered, and this finding raises an alarm regarding the need to evaluate whether CT findings remain consistent or change when new variants appear.

In press

Acknowledgement

The authors gratefully acknowledge the expert biostatistician, Myoung-Jin Jang (Seoul National University Hospital Medical Research Collaborating Center) for the review of statistical analysis and Andrew Dombrowski, PhD (Compecs, Inc.) for his assistance in improving the use of English in this manuscript.

In press

References

1. Walensky RP, Walke HT, Fauci AS. SARS-CoV-2 Variants of Concern in the United States-Challenges and Opportunities. JAMA 2021;325(11):1037-1038. doi: 10.1001/jama.2021.2294

2. Tao K, Tzou PL, Nouhin J, et al. The biological and clinical significance of emerging SARS-CoV-2 variants. Nat Rev Genet 2021;22(12):757-773. doi: 10.1038/s41576-021-00408-x

3. Harvey WT, Carabelli AM, Jackson B, et al. SARS-CoV-2 variants, spike mutations and immune escape. Nat Rev Microbiol 2021;19(7):409-424. doi: 10.1038/s41579-021-00573-0

4. Lopez Bernal J, Andrews N, Gower C, et al. Effectiveness of Covid-19 Vaccines against the B.1.617.2 (Delta) Variant. N Engl J Med 2021;385(7):585-594. doi: 10.1056/NEJMoa2108891

5. Del Rio C, Malani PN, Omer SB. Confronting the Delta Variant of SARS-CoV-2, Summer 2021. JAMA 2021;326(11):1001-1002. doi: 10.1001/jama.2021.14811

6. Li B, Deng A, Li K, et al. Viral infection and transmission in a large, well-traced outbreak caused by the SARS-CoV-2 Delta variant. Nat Commun 2022;13(1):460. doi: 10.1038/s41467-022-28089-y

7. Butt AA, Dargham SR, Chemaitelly H, et al. Severity of Illness in Persons Infected With the SARS-CoV-2 Delta Variant vs Beta Variant in Qatar. JAMA Intern Med 2022;182(2):197-205. doi: 10.1001/jamainternmed.2021.7949

8. Iuliano AD, Brunkard JM, Boehmer TK, et al. Trends in Disease Severity and Health Care Utilization During the Early Omicron Variant Period Compared with Previous SARS-CoV-2 High Transmission Periods - United States, December 2020-January 2022. MMWR Morb Mortal Wkly Rep 2022;71(4):146-152. doi: 10.15585/mmwr.mm7104e4

9. Ulloa AC, Buchan SA, Daneman N, Brown KA. Estimates of SARS-CoV-2 Omicron Variant Severity in Ontario, Canada. JAMA 2022. doi: 10.1001/jama.2022.2274

10. Wolter N, Jassat W, Walaza S, et al. Early assessment of the clinical severity of the SARS-CoV-2 omicron variant in South Africa: a data linkage study. Lancet 2022;399(10323):437-

In press

446. doi: 10.1016/S0140-6736(22)00017-4

11. Rubin GD, Ryerson CJ, Haramati LB, et al. The Role of Chest Imaging in Patient Management during the COVID-19 Pandemic: A Multinational Consensus Statement from the Fleischner Society. Radiology 2020;296(1):172-180. doi: 10.1148/radiol.2020201365

12. Kwee TC, Kwee RM. Chest CT in COVID-19: What the Radiologist Needs to Know. RadioGraphics 2020;40(7):1848-1865. doi: 10.1148/rg.2020200159

13. Hui KPY, Ho JCW, Cheung MC, et al. SARS-CoV-2 Omicron variant replication in human bronchus and lung ex vivo. Nature 2022. doi: 10.1038/s41586-022-04479-6

14. Korea COVID-19 update Korea Disease Control and Prevention Agency. https://www.kdca.go.kr/board/board.es?mid=a20501010000&bid=20501010015. Accessed on Mar 212, 2022.

15. Bernheim A, Mei X, Huang M, et al. Chest CT Findings in Coronavirus Disease-19 (COVID-19): Relationship to Duration of Infection. Radiology 2020;295(3):200463. doi: 10.1148/radiol.2020200463

16. Simpson S, Kay FU, Abbara S, et al. Radiological Society of North America Expert Consensus Document on Reporting Chest CT Findings Related to COVID-19: Endorsed by the Society of Thoracic Radiology, the American College of Radiology, and RSNA. Radiology: Cardiothoracic Imaging 2020;2(2):e200152. doi: 10.1148/ryct.2020200152

17. Wang Y, Dong C, Hu Y, et al. Temporal Changes of CT Findings in 90 Patients with COVID-19 Pneumonia: A Longitudinal Study. Radiology 2020;296(2):E55-E64. doi: 10.1148/radiol.2020200843

18. Yoo SJ, Yoon SH, Lee JH, et al. Automated Lung Segmentation on Chest Computed Tomography Images with Extensive Lung Parenchymal Abnormalities Using a Deep Neural Network. Korean J Radiol 2021;22(3):476-488. doi: 10.3348/kjr.2020.0318

19. Yoo S, Qi X, Inui S, et al. Deep Learning-Based Automatic CT Quantification of

Coronavirus Disease 2019 Pneumonia: An International Collaborative Study. J Comput Assist Tomogr. 2022 May-Jun 01;46(3):413-422.

20. Nam JG, Witanto JN, Park SJ, Yoo SJ, Goo JM, Yoon SH. Automatic pulmonary vessel segmentation on noncontrast chest CT: deep learning algorithm developed using spatiotemporally matched virtual noncontrast images and low-keV contrast-enhanced vessel maps. Eur Radiol 2021;31(12):9012-9021. doi: 10.1007/s00330-021-08036-z

21. Isensee F, Jaeger PF, Kohl SAA, Petersen J, Maier-Hein KH. nnU-Net: a self-configuring method for deep learning-based biomedical image segmentation. Nat Methods 2021;18(2):203-211. doi: 10.1038/s41592-020-01008-z

22. Choi H, Qi X, Yoon SH, et al. Extension of Coronavirus Disease 2019 on Chest CT and Implications for Chest Radiographic Interpretation. 2020;2(2):e200107. doi: 10.1148/ryct.2020200107

23. Lins M, Vandevenne J, Thillai M, et al. Assessment of Small Pulmonary Blood Vessels in COVID-19 Patients Using HRCT. Acad Radiol 2020;27(10):1449-1455. doi: 10.1016/j.acra.2020.07.019

24. Thillai M, Patvardhan C, Swietlik EM, et al. Functional respiratory imaging identifies redistribution of pulmonary blood flow in patients with COVID-19. Thorax 2021;76(2):182-184. doi: 10.1136/thoraxjnl-2020-215395

25. Jaegere TMHd, Krdzalic J, Fasen BACM, Kwee RM, group C-CIS-ENs. Radiological Society of North America Chest CT Classification System for Reporting COVID-19 Pneumonia: Interobserver Variability and Correlation with Reverse-Transcription Polymerase Chain Reaction. Radiology: Cardiothoracic Imaging 2020;2(3):e200213. doi: 10.1148/ryct.2020200213

26. Inui S, Kurokawa R, Nakai Y, et al. Comparison of Chest CT Grading Systems in COVID-

In press

19 Pneumonia. Radiology: Cardiothoracic Imaging 2020;2(6):e200492. doi: 10.1148/ryct.2020200492

27. Miranda Magalhães Santos JM, Paula Alves Fonseca A, Pinheiro Zarattini Anastacio E, Formagio Minenelli F, Furtado de Albuquerque Cavalcanti C, Borges da Silva Teles G. Initial Results of the Use of a Standardized Diagnostic Criteria for Chest Computed Tomography Findings in Coronavirus Disease 2019. Journal of Computer Assisted Tomography 2020;44(5):647-651. doi: 10.1097/rct.0000000000001054

28. Hammer MM. Real-World Diagnostic Performance of RSNA Consensus Reporting Guidelines for Findings Related to COVID-19 on Chest CT. AJR Am J Roentgenol 2022;218(1):75-76. doi: 10.2214/AJR.21.26560

29. Lee JE, Hwang M, Kim Y-H, et al. Imaging and Clinical Features of COVID-19 Breakthrough Infections: A Multicenter Study. Radiology 2022;0(0):213072. doi: 10.1148/radiol.213072

30. Estepar RS, Kinney GL, Black-Shinn JL, et al. Computed tomographic measures of pulmonary vascular morphology in smokers and their clinical implications. Am J Respir Crit Care Med 2013;188(2):231-239. doi: 10.1164/rccm.201301-0162OC

31. Morris MF, Pershad Y, Kang P, et al. Altered pulmonary blood volume distribution as a biomarker for predicting outcomes in COVID-19 disease. Eur Respir J 2021;58(3). doi: 10.1183/13993003.04133-2020

32. Halawa S, Pullamsetti SS, Bangham CRM, et al. Potential long-term effects of SARS-CoV-2 infection on the pulmonary vasculature: a global perspective. Nat Rev Cardiol 2021. doi: 10.1038/s41569-021-00640-2

33. Ackermann M, Verleden SE, Kuehnel M, et al. Pulmonary Vascular Endothelialitis, Thrombosis, and Angiogenesis in Covid-19. N Engl J Med 2020;383(2):120-128. doi: 10.1056/NEJMoa2015432

In press

34. Suh YJ, Hong H, Ohana M, et al. Pulmonary Embolism and Deep Vein Thrombosis in COVID-19: A Systematic Review and Meta-Analysis. Radiology 2021;298(2):E70-E80. doi: 10.1148/radiol.2020203557

35. Wilkinson E. Covid-19: We have good treatments for omicron, but questions remain, say doctors. BMJ 2022 11;376:o61. doi: 10.1136/bmj.o61

In press

Tables

Table 1: Clinical Characteristics of Patients with COVID-19 according to the Variants

Clinical characteristic	Delta variant (n=88)	Omicron variant (n=88)	*P* value
Age (y)	67±15	62±19	.06
Men	46 (52%)	51 (58%)	.55
Presence of comorbidities*	73 (83%)	67 (76%)	.35
Vaccination status			<.001
Unvaccinated	28 (32%)	25 (28%)	
Partially vaccinated	5 (6%)	4 (5%)	
Fully vaccinated	55 (62%)	20 (23%)	
Booster vaccinated	0 (0%)	39 (44%)	
Infection duration (days)**			
Pre-symptomatic	9 (10%)	3 (3%)	.009
0-2 days	22 (25%)	31 (35%)	
3-5 days	24 (27%)	38 (43%)	
6-11 days	26 (30%)	13 (15%)	
>11 days	7 (8%)	3 (3%)	
Complete blood count (cells/μL)	5920±3063	6479±3037	.23
Lymphocyte count (/μL)	1160±656	1324±627	.09
Lactate dehydrogenase (U/L)	555±213	513±214	.21
Oxygen treatment	27 (31%)	24 (27%)	.74
30-day composite outcome†	7 (8%)	12 (14%)	.33

* Comorbidities included obesity, cardiovascular or cerebrovascular disease, immunocompromised status, diabetes mellitus, and chronic lung, liver, or renal disease.

**Infection duration was defined as days from symptom onset to the CT scan.

† The composite outcome was defined as any of the following events: oxygen ventilation, intensive care unit admission, or mortality.

In press

Table 2: Findings on Chest CT Scans of Patients with COVID-19, According to Variant

Finding	Delta variant (n=88)	Omicron variant (n=88)	*P* value
RSNA COVID-19 imaging classification*			.004
Typical appearance	50 (57%)	28 (32%)	
Indeterminate appearance	18 (20%)	27 (31%)	
Atypical appearance	3 (3%)	11 (13%)	
Negative for pneumonia	17 (19%)	22 (25%)	
Score by visual assessment of pneumonia extent†	7.7±6.6	5.4±6.0	.02
Right upper lobe	1.3±1.3	1.0±1.3	.06
Right middle lobe	1.2±1.3	0.9±1.3	.08
Right lower lobe	1.8±1.5	1.4±1.5	.06
Left upper lobe	1.5±1.4	1.0±1.2	.005
Left lower lobe	1.9±1.6	1.3±1.5	.01
Visual assessment of pneumonia density‡**			.61
Predominant GGO	47 (66%)	45 (68%)	
Predominant consolidation	6 (8%)	8 (12%)	
Mixed pattern	18 (25%)	13 (20%)	
Visual assessment of predominant distribution**			<.001
Peri-bronchovascular predilection	5 (7%)	25 (38%)	
Subpleural predilection	43 (61%)	22 (33%)	
Mixed pattern	23 (32%)	19 (29%)	
Visual assessment for lymphadenopathy§	13 (15%)	10 (11%)	.66
Visual assessment for presence of pleural effusion	19 (22%)	16 (18%)	.71
Mean CT value (Hounsfield units)	-402±115	-404±139	.92
Pneumonia extent by quantitative CT analysis	7% ±11	5% ±10	.14
Right upper lobe	5% ±10	3% ±8	.20
Right middle lobe	4% ±9	3% ±9	.38
Right lower lobe	11% ±9	9% ±18	.47
Left upper lobe	5% ±10	3% ±8	.16
Left lower lobe	11% ±16	9±18	.50
Pneumonia weight by quantitative CT analysis	143g ±191	95g ±174	.09
Vessel smaller than 5 mm^2	44% ±8	48% ±11	.004
Pleural effusion amount (mL)	149±264	275±407	.47

Note—RSNA: Radiological Society of North America; GGO: ground-glass opacity

* The RSNA classification of COVID-19 on chest CT - typical appearance: peripheral bilateral ground-glass opacities (GGOs) or multifocal round GGOs with or without consolidation or intralobular lines, or reverse halo sign; indeterminate appearance: presence of GGOs with or without consolidation, but absence of typical features; atypical appearance: absence of typical or indeterminate features with presence of lobar/segmental consolidation without GGOs, discrete centrilobular nodules, lung cavitation, or smooth interlobular septal thickening with pleural effusion; negative for pneumonia: no CT features to suggest pneumonia.

In press

** The pneumonia density and predominant distribution were evaluated in cases with pneumonia (Delta variant, n=71; Omicron variant, n=66).

† The total CT score was the sum of the individual lobar scores (each of the five lung lobes was visually scored on a scale of 0 to 5, with 0 indicating no involvement; 1, less than 5% involvement; 2, 5%–25% involvement; 3, 26%–49% involvement; 4, 50%–75% involvement; and 5, more than 75% involvement).

‡ Pneumonia density was assessed in patients with pneumonia (n=71 with the Delta variant; n=66 with the Omicron variant); predominant GGO: GGO to consolidation ratio ≥2/3; predominant consolidation: GGO to consolidation ratio <1/3; mixed pattern: 1/3 ≤GGO to consolidation ratio <2/3.

§ Lymphadenopathy was considered present when mediastinal, interlobar, or supraclavicular lymph nodes were enlarged ≥ 1 cm in their short axis.

In press

Table 3: Impact of Omicron Variant Compared to Delta Variant on RSNA CT Classification System, CT Severity, Peripheral Vascularity, and the Composite Outcome

Statistical analysis and dependent variables	Univariable analysis		Multivariable analysis	
Logistic regression analysis	**Odds ratio**	***P* value**	**Odds ratio**	***P* value**
Typical CT appearance for COVID-19*	0.36 (0.19, 0.66)	.001	0.34 (0.16, 0.74)	.006
Peri-bronchovascular predilection*	8.1 (2.9, 23)	<.001	9.2 (2.9, 29)	<.001
Linear regression analysis	**β value**		**β value**	
Visual extent	-2.3 (-4.2, -0.42)	.02	-1.09 (-2.6, 0.46)*	.17
Pneumonia volume (%)	-2.3 (-5.4, 0.79)	.14	-0.62 (-3.4, 2.2)*	.67
Pneumonia weight (g)	-47 (-113, 20)	.17	-6.9 (-67, 53)*	.82
BV5% (%)	4.4 (1.4, 7.4)	.004	3.8 (0.92, 6.8)**	.01
Cox regression analysis	**Hazard ratio**		**Hazard ratio**	
30-day composite outcome (adjusted with visual extent)	1.83 (0.72, 4.7)	.21	3.08 (0.78, 12)***	.11
30-day composite outcome (adjusted with volume)			2.37 (0.48, 11)****	.29

Note— BV5%: the percentage of blood volume in intrapulmonary vessels with a cross-sectional area <5 mm^2 relative to the total pulmonary blood volume; The composite outcome comprised the occurrence of oxygen ventilation, intensive care unit admission, or mortality; RSNA: Radiological Society of North America. Data in parenthesis are 95% confidence intervals.

*Adjusted for age, comorbidities, infection duration, and vaccination history. The proportion of a typical CT appearance also was greater with older age (*P*=.006) and longer infection duration (six days or longer: *P*<.001 to .004), but was lower with full vaccination (*P*=.006) in the multivariable analysis. In addition, the visual extent, pneumonia volume, and pneumonia weight was greater with age (*P*<.001 to .009) and longer infection duration (all *P*<.001), but was lower with full vaccination (*P*<.001 to 0.084) in the multivariable analyses.

**Adjusted for age, comorbidities, infection duration, vaccination history, and pneumonia volume. The BV5% also was lower as pneumonia volume was greater (*P*=.001).

***Adjusted for age, comorbidities, infection duration, vaccination history, lymph node enlargement, pleural effusion, lymphocyte count, lactate dehydrogenase level, and

visual pneumonia extent. A greater visual extent was the sole predictor of developing the 30-day composite outcome (*P*=.002) in the multivariable analysis.

****Adjusted for age, comorbidity, infection duration, vaccination history, lymph node enlargement, pleural effusion, lymphocyte count, lactate dehydrogenase level, pneumonia volume, and BV5%. A larger pneumonia volume (*P*=.002) and a higher lactate dehydrogenase level (*P*=.035) were predictors of developing the 30-day composite outcome in the multivariable analysis.

In press

Figures

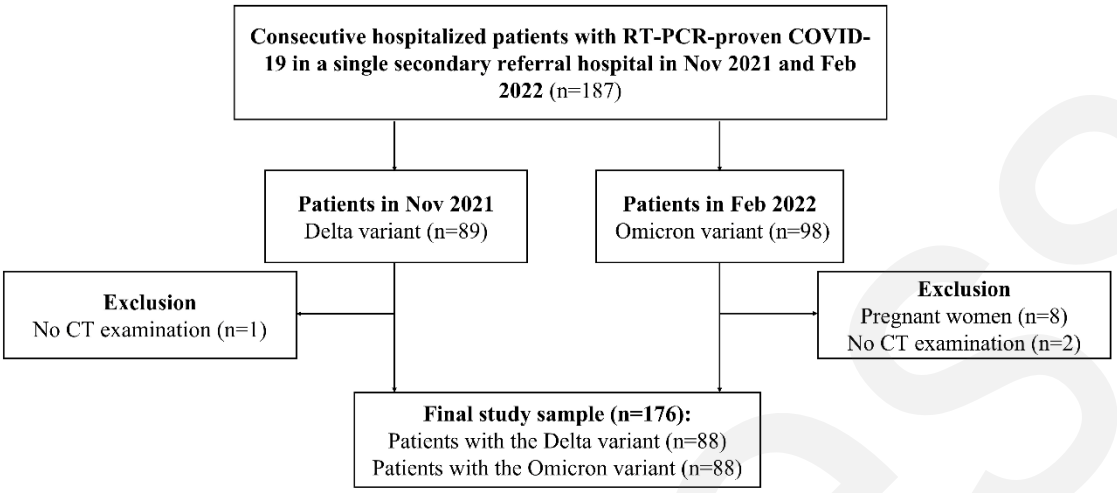

Figure 1: Flowchart of patient inclusion. RT-PCR: real-time reverse-transcription polymerase chain reaction assay.

In press

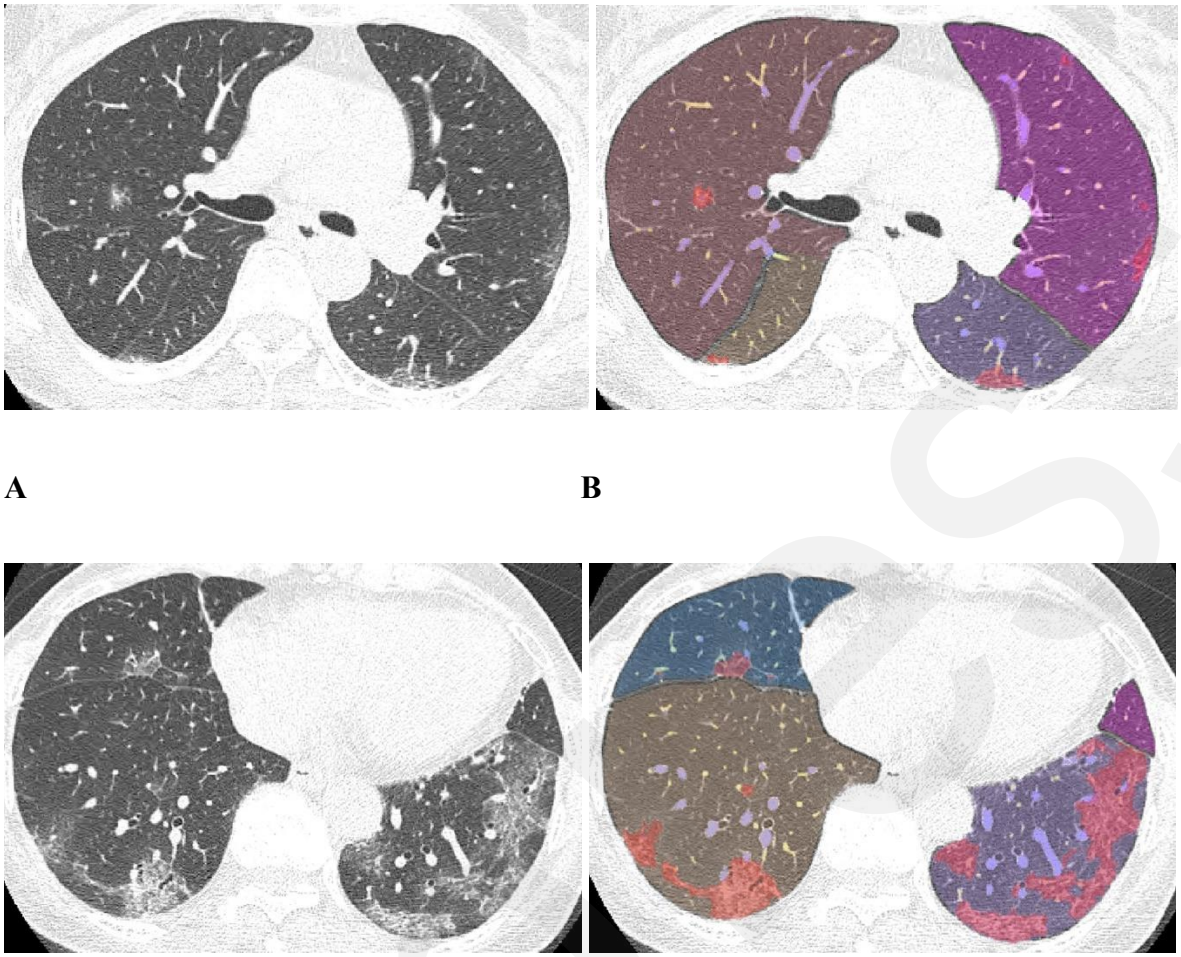

A **B**

C **D**

Figure 2: Chest CT from a 66-year-old woman with the Delta variant of COVID-19 with a typical CT appearance.

Unenhanced axial CT images **(A, B)** show peripheral bilateral ground-glass opacities with some intralobular lines predominantly involving both lower lobes. Segmentation overlay images **(C, D)** show the segmentation results of pneumonia (red), lobes (orange to violet), and pulmonary vessels with a cross-sectional area <5 mm^2 (yellow) and ≥5 mm^2 (blue). The visual CT score was 12 points, and the pneumonia volume was 9%.

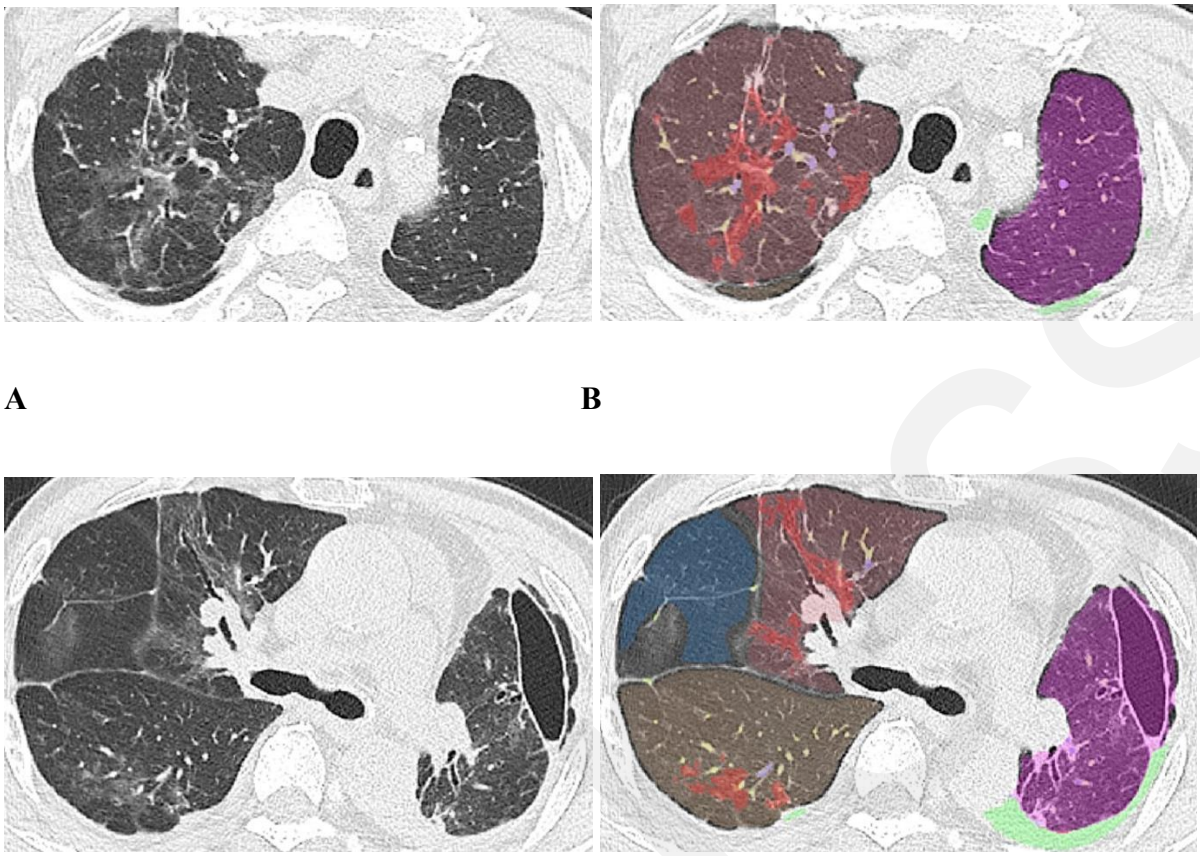

A **B**

C **D**

Figure 3: Chest CT from a 77-year-old male with the Omicron variant of COVID-19 with indeterminate CT appearance.

Unenhanced axial CT images **(A, B)** show unilateral peri-bronchovascular ground-glass opacities without intralobular lines or an apicobasal predilection. Segmentation overlay images **(C, D)** show the segmentation results of pneumonia (red), lobes (orange to violet), effusion (light green), and pulmonary vessels with a cross-sectional area <5 mm^2 (yellow) and ≥5 mm^2 (blue). The visual CT score was 13 points, and the pneumonia volume was 8%. A focal ground-glass opacity in the lateral portion of left bottom image (D) was not included in the pneumonia mask as it was the minor fissure between right upper and middle lobes.

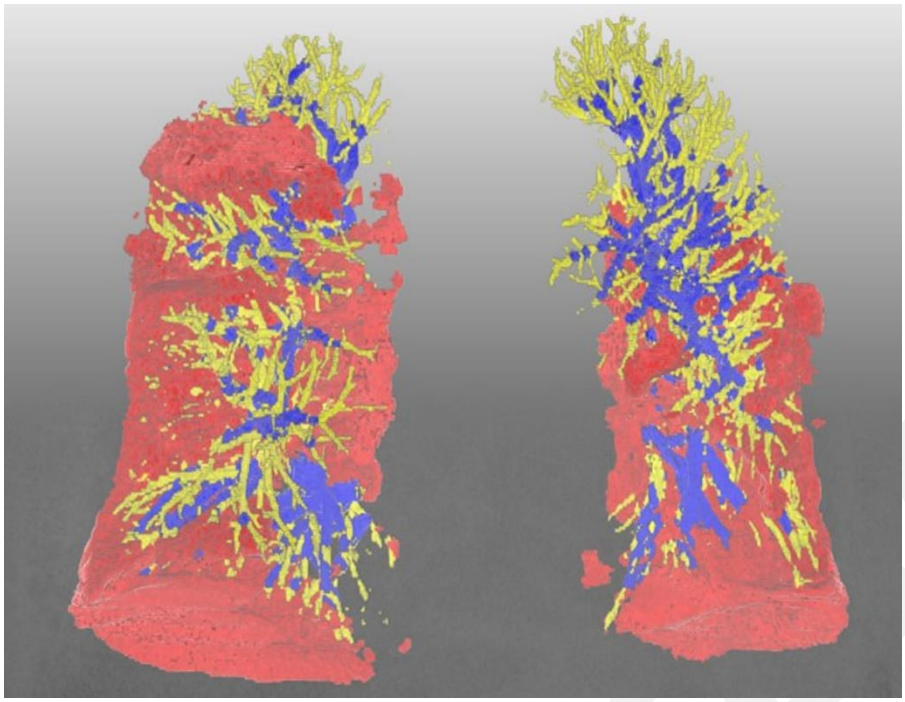

Figure 4: Chest CT from an 88-year-old woman with the Delta variant.

A representative three-dimensional image shows lower-lobe predominant pneumonia (pneumonia volume, 14.7%) and a lower percentage of blood volume in intrapulmonary vessels with a cross-sectional area <5 mm^2 relative to the total pulmonary blood volume (34.6%). The blue vessels have a cross-sectional area ≥5 mm^2, while the yellow vessels have a cross-sectional area <5 mm^2. The red indicates COVID-19 pneumonia.

In press

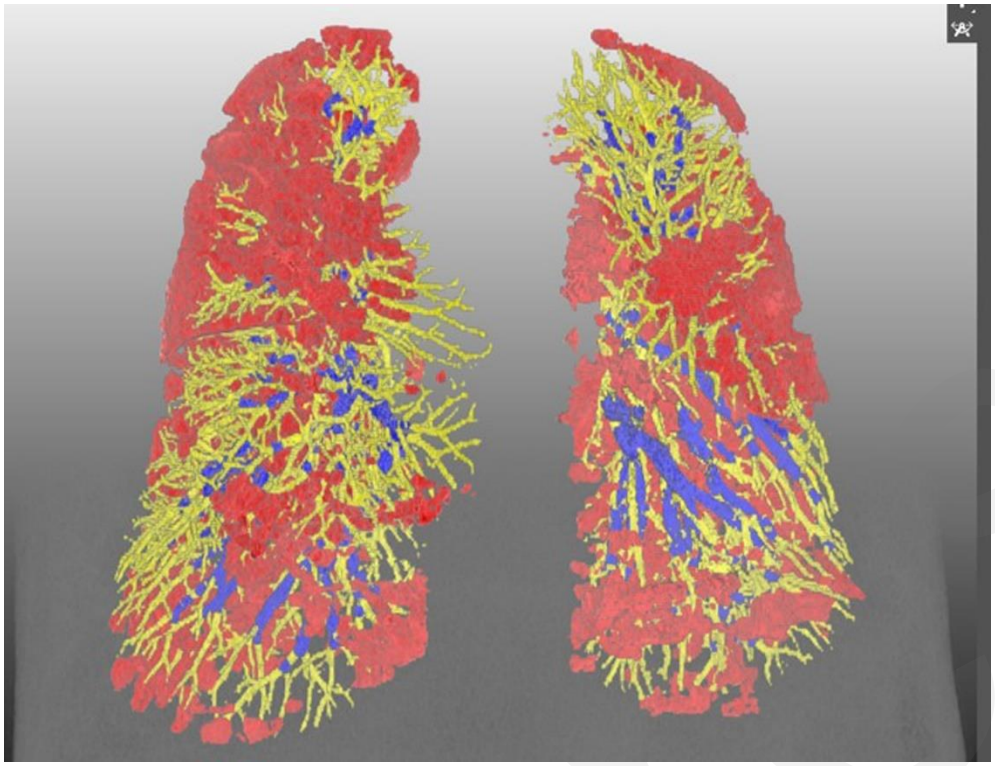

Figure 5: Chest CT from a 52-year-old male with the Omicron variant.

A representative three-dimensional image shows pneumonia evenly affecting lungs (pneumonia volume, 17.5%) and a preserved percentage of blood volume in intrapulmonary vessels with a cross-sectional area <5 mm^2 relative to the total pulmonary blood volume (51.5%). The blue vessels have a cross-sectional area ≥5 mm^2, while the yellow vessels have a cross-sectional area <5 mm^2. The red indicates COVID-19 pneumonia.

In Press

Appendix E1

Study sample

In Korea, when patients with COVID-19 with a positive real-time reverse-transcription polymerase chain reaction assay for SARS-CoV-2 were identified, local public health authorities triaged them according to risk factors and severity in the national guideline. The authorities referred high-risk or symptomatic patients to community treatment centers or designated hospitals. The risk factors for progression in the national guideline were as follows:

- Age ≥60 years
- Symptoms that require attention: loss of consciousness, shortness of breath (holding breath at rest or even when moving for short distances), fever (>38°C)
- Chronic underlying disease: uncontrolled diabetes mellitus, chronic kidney disease or patients requiring hemodialysis, chronic lung disease (chronic obstructive pulmonary disease, asthma, etc.), heart failure or coronary artery disease, cancer patients undergoing chemotherapy, organ transplantation, patients taking immunosuppressive drugs, bed-ridden (those who lie down more than 50% of the day)
- Special circumstances: those who need special care such as mentally ill, pregnant women

The collected clinico-laboratory information included age, sex, comorbidities, infection duration at the time of the CT scan, vaccination history, basic laboratory results, the need for oxygen therapy, and outcomes. The comorbidities comprised obesity, cardiovascular or cerebrovascular disease, immunocompromised status, diabetes mellitus, and chronic lung, liver, or renal disease. The laboratory tests included a complete blood count, lymphocyte count, and lactate dehydrogenase.

In press

CT acquisition

All chest CT scans were obtained at full inspiration using one of the following 24- or higher-channel CT scanners: Aquilion ONE (n=156) (Canon Medical Systems); Revolution CT (n=14), Revolution Maxima (n=1), Revolution EVO (n=1) (GE Healthcare); SOMATOM Definition AS+ (n=1), SOMATOM Scope (n=1), SOMATOM Definition Edge (n=1), and Sensation Open (n=1) (Siemens Healthcare). Most CT scans were conducted using a low-dose protocol (118 of 176; 67%) and a setting of 120 kV (169 of 176; 96%) without iodinated medium (165 of 176; 94%), and almost all scans were reconstructed with sections of 1.25 mm or thinner (171 of 176; 97%) without section gap using a sharp reconstruction kernel (162 of 176; 92%). Median CT dose index volume and dose-length product were 21.9 mGy (interquartile range, 13.7-22.8) and 559.3 mGy*cm (interquartile range, 406.3-746.9), respectively.

Visual CT analysis

The four categories in the Radiological Society of North America (RSNA) Expert Consensus Document (1) were defined as follows: typical, peripheral, bilateral, ground-glass opacity [GGO], or multifocal GGO of rounded morphology with or without consolidation or visible intralobular lines; reverse halo sign or other findings of organizing pneumonia), indeterminate (absence of typical features and presence of multifocal, diffuse, perihilar, or unilateral GGO with or without consolidation lacking a specific distribution and non-rounded or non-peripheral in morphology; few very small GGOs with a non-rounded and non-peripheral distribution), atypical (absence of typical or indeterminate features and presence of isolated lobar or segmental consolidation without GGO; discrete small nodules; lung cavitation; smooth

In press

interlobular septal thickening with pleural effusion), and negative for pneumonia (no CT features suggestive of pneumonia).

Pneumonia density was visually evaluated as predominant GGO (GGO to consolidation ratio ≥2/3), predominant consolidation (GGO to consolidation ratio <1/3), and a mixed pattern (1/3 ≤ GGO to consolidation ratio <2/3). The distribution of COVID-19 pneumonia were classified into three patterns: peri-bronchovascular predilection, subpleural predilection, and mixed pattern. Lymphadenopathy was considered present when mediastinal, interlobar, or supraclavicular lymph nodes were enlarged ≥ 1 cm in their short axis. The presence of pleural effusion was also evaluated.

Quantitative CT analysis

The segmentation results of 22 out of 176 CT scans required revision and main reason for the revision was the incorrect inclusion of effusion into the lung mask; this was simply corrected by performing subtraction using the effusion mask. Five patients with SARS-CoV-2 (one patient with Delta and four patients with Omicron variant) were excluded from this quantitative analysis due to the presence of substantial respiratory artifacts on CT images.

Statistical analyses.

After adjusting for age, comorbidities, vaccination, and infection duration, multivariable logistic regression analysis was performed to examine the association between the variants and CT category. Multivariable linear regression analyses were performed to examine the relationships between the variants and visual CT extent, pneumonia percentage, weight with the same adjustment. BV5% was additionally adjusted for pneumonia volume.

In press

Multivariable Cox regression analyses were conducted to evaluate the association between the variants and the composite outcome while adjusting age, comorbidity, infection duration, vaccination history, lymph node enlargement, pleural effusion, lymphocyte count, lactate dehydrogenase level, along with either visual extent or volume parameters (pneumonia volume and BV5%).

We did not count boosters separately in the analyses and merged patients who had received boosters with the category of full vaccination, as boosters were exclusively received by patients in the Omicron group.

In press

Supplemental Reference

1. Jaegere TMHd, Krdzalic J, Fasen BACM, Kwee RM, group C-CIS-ENs. Radiological Society of North America Chest CT Classification System for Reporting COVID-19 Pneumonia: Interobserver Variability and Correlation with Reverse-Transcription Polymerase Chain Reaction. Radiology: Cardiothoracic Imaging 2020;2(3):e200213. doi: 10.1148/ryct.2020200213

In press

Supplemental Figure

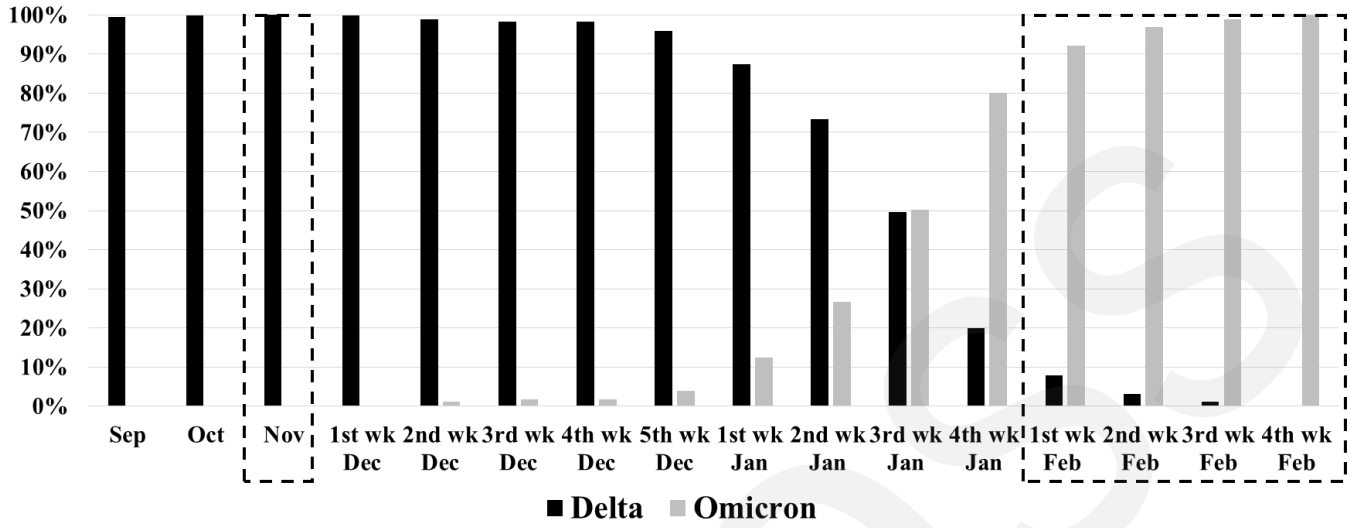

Figure E1: A nationwide trend of predominant variants of SARS-CoV-2 between September 2021 and February 2022.

Since the pandemic, Korea has been conducting genomic surveillance in five representative laboratory centers that geographically cover the entire nation to monitor predominant variants of COVID-19. The centers run whole-genome sequencing and sequencing S protein receptor-binding domain and update the trend of predominant variants weekly. Test specimens approximately cover one-fifths of all RT-PCR positive specimens for SARS-CoV-2. The Delta variant started to be replaced by the Omicron variant from December 2021 through January 2022.

In press